

## Hydrothermal Synthesis of Single-Crystalline Antimony Telluride Nanobelts

Weidong Shi, Jiangbo Yu, Haishui Wang, and Hongjie Zhang\*

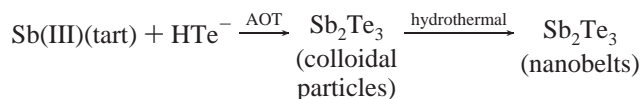
Key Laboratory of Rare Earth Chemistry and Physics, Changchun Institute of Applied Chemistry, and Graduate School of the Chinese Academy of Sciences, Chinese Academy of Sciences, Changchun 130022, China

Received September 27, 2006; E-mail: hongjie@ns.ciac.jl.cn

Since the discovery of semiconducting oxide nanobelts in 2001, beltlike nanomaterials have attracted considerable attention due to their distinctive geometries, novel physical and chemical properties, and potential applications in numerous areas such as nanoscale electronics and photonics.<sup>1–4</sup> As a consequence, highly anisotropic nanobelts using various materials, such as oxides (ZnO, SnO<sub>2</sub>, and VO<sub>2</sub>(B)),<sup>1</sup> sulfides (ZnS and CdS),<sup>2</sup> selenides (ZnSe and CdSe),<sup>3</sup> element (Au, C, and Te),<sup>4</sup> and some other compounds (SiC and Pb<sub>3</sub>O<sub>2</sub>Cl<sub>2</sub>),<sup>5</sup> etc., have been fabricated through a variety of methods. However, to the best of our knowledge, no studies have been reported on the preparation of semiconducting telluride nanobelts to date, although their preparation is strongly desired.

Antimony telluride (Sb<sub>2</sub>Te<sub>3</sub>) is a kind of thermoelectric material with the high figure of merit (ZT). It has attracted considerable fundamental and technological interests for decades because of its potential applications in minipower-generation systems and micro-coolers, CCD technology, and infrared detectors.<sup>6</sup> Both theoretical prediction and experimental investigation have suggested that nanostructuring the thermoelectric materials can be considered as a successful strategy to gain factorial enhancements in ZT due to both a high density of states and an increased phonon scattering or reduced lattice thermal conductivity in nanosystems.<sup>7</sup> The Sb<sub>2</sub>Te<sub>3</sub> crystals have been transferred into nanometer scale (such as nanowires, nanoplates, and nanofilms) through various chemical methods,<sup>8</sup> including solvothermal process, colloidal route, decomposing a single-source precursor, electrochemical deposition into porous alumina, and electrochemical atomic layer epitaxy. Recent studies verify that green and mild surfactant-assisted hydrothermal processes have extraordinary ability in the fabrication of the 1D beltlike nanostructures.<sup>9</sup> Here, on the basis of the above considerations, we developed a novel hydrothermal approach employing the anionic surfactant sodium bis(2-ethylhexyl)sulfosuccinate (AOT) for the synthesis of single-crystalline Sb<sub>2</sub>Te<sub>3</sub> nanobelts.

The synthesis route can be shown as follows:



In a typical synthesis, 0.013 g of Te power and 0.025 g of NaBH<sub>4</sub> were taken into a 50 mL three-neck round-bottom flask. The flask was purged with N<sub>2</sub> flow thoroughly and heated to 80 °C. Five milliliters of deionized water was injected into the flask under constant stirring. Thirty minutes later, all Te power dissolved. The pink-color NaHTe solution was first prepared. Then 10 mL of AOT (0.6 g) aqueous solution was injected into the fresh NaHTe solution. After the resulting solution had been stirred for 20 min, 3 mL of SbCl<sub>3</sub> (0.022 g) and tartaric acid (0.07 g) aqueous solution was injected into the reaction vessel. The resulting black colloid was stirred vigorously for 15 min and then transferred into a Teflon-lined stainless-steel autoclave of 20 mL capacity, which was filled

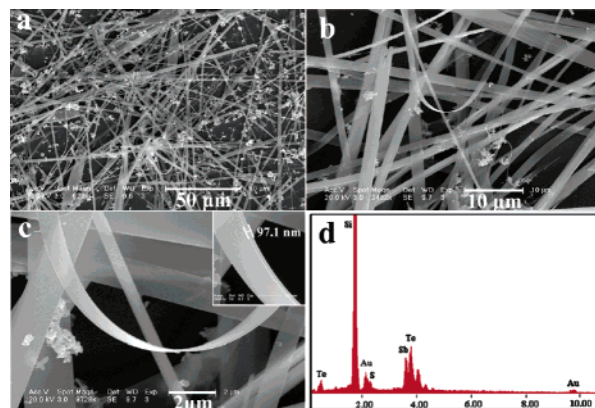


**Figure 1.** SEM images of Sb<sub>2</sub>Te<sub>3</sub> nanobelts: (a) low magnification; (b) and (c) high magnification; (d) EDS pattern which indicates the belts are composed of Sb<sub>2</sub>Te<sub>3</sub>.

in ca. 80% of the total volume. The tank was maintained at 200 °C for 24 h and then cooled to room temperature. The black products were collected by centrifuge, washed several times using distilled water and absolute ethanol, and dried under vacuum at 50 °C for 2 h.

The morphology and size of the as-synthesized products on Au-coated silicon substrate were characterized by field-emission scanning electron microscopy (FESEM, XL30 ESEM FEG, Figure 1). The low-magnification FESEM image (Figure 1a) reveals that the typical products consist of a large quantity of beltlike structures with the lengths in the range of several tens to several hundred micrometers. The high-magnification FESEM images (Figure 1b and 1c) show that the width of belts is ca. 1–3 μm, and their thickness is quite thin, about 100 nm. The chemical composition of these nanobelts was further determined by energy-dispersive X-ray spectroscopy (EDS, Figure 1d). Besides the elements Au and Si from substrate, peaks of the elements Sb, Te, and S are detected in the EDS pattern. The appearance of element S should be attributed to a small quantity of rudimental AOT. The phase purity of the products was examined on a Rigaku-D/max 2500V X-ray diffractometer (XRD) with Cu Kα radiation (λ = 1.5418 Å). The diffraction peaks in Figure 2 can be indexed to the rhombohedral phase of Sb<sub>2</sub>Te<sub>3</sub> [space group:  $R\bar{3}m$  (No. 166)] with lattice constants  $a = 4.264 \text{ Å}$  and  $c = 30.458 \text{ Å}$  (JCPDS 65-3678). The peaks marked with an asterisk are possibly from some other Sb–Te compounds.

Transmission electron microscopy (TEM) and high-resolution TEM (HRTEM, H-9000NAR at 300 kV) provide further insight into the microstructural details of beltlike nanostructures. Figure 3a shows the TEM image of a typical single nanobelt. The selected area electron diffraction (SAED) taken from the edge of this nanobelt in Figure 3b can be indexed as a rhombohedral antimony telluride crystal recorded from the [110] zone axis. Figure 3c shows a representative HRTEM image of the edge area of the Sb<sub>2</sub>Te<sub>3</sub>

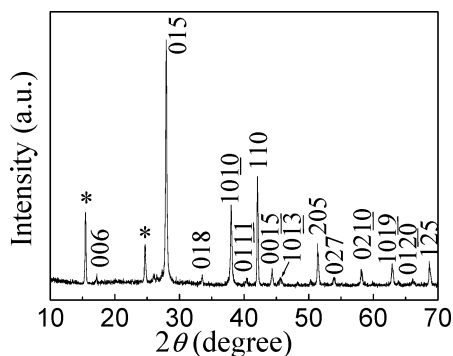


Figure 2. XRD pattern of the obtained product.

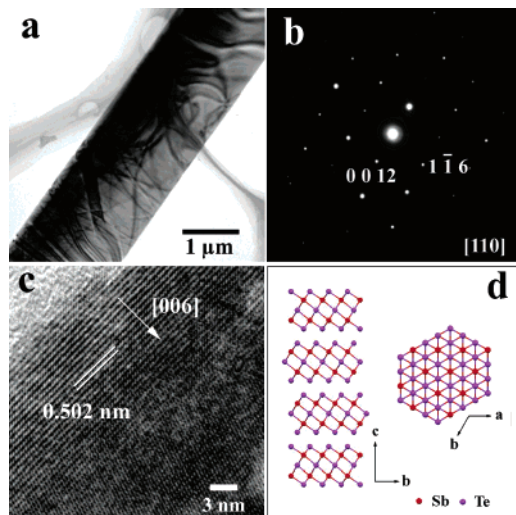


Figure 3. (a) TEM image, (b) SAED pattern, and (c) HRTEM image of a single  $\text{Sb}_2\text{Te}_3$  nanobelt. (d) Crystal structure of  $\text{Sb}_2\text{Te}_3$ .

nanobelt. This image reveals that the nanobelt is single-crystalline with interplanar spacing of about 0.502 nm, which corresponds to the (006) crystalline plane. It indicates that the growth direction of the nanobelts is along the *a*- or *b*-axis.

In the process of the synthesis, the introduction of tartaric acid can make  $\text{SbCl}_3$  completely dissolve in water because they can form the diffuent complex  $\text{Sb(III)(tart)}$ . Further studies suggest that the surfactant AOT plays a key role in the formation of the beltlike nanostructures.  $\text{Sb}_2\text{Te}_3$  crystal has 15 layers stacked along the *c*-axis and presents the combination of three hexagonal layer stacks of composition in which each set consists of five atoms ( $\text{Te}_1\text{-Sb-Te}_2\text{-Sb-Te}_1$ ). Between two adjacent  $\text{Te}_1$  layers, there are van der Waals bonds, while all others are covalent bonds. This special bonding structure leads to the faster growth of crystal along the top–bottom crystalline plane compared with that along the *c*-axis, which makes them tend to form platelike morphology. In our case, the obtained products without adding AOT consist only of irregular nanoplates. The diameter of the nanoplates is about 100–300 nm, and their thickness is several tens of nanometers. When the amount of AOT is increased to 0.2 g, we find that some beltlike  $\text{Sb}_2\text{Te}_3$  nanostructures begin to appear, though the nanoplates still dominate in the products. It is reasonable to indicate that the nanobelts' growth is due to specific interactions between the surfactant AOT and  $\text{Sb}_2\text{-Te}_3$  colloidal particles. In the synthesis of inorganic nanostructures, many organic additives have been used to modify certain crystal-

lographic surfaces. The absorption of the organic additives on those surfaces will eliminate part of the dangling bond and result in the reduction of their surface energy and, therefore, suppress the growth along these surfaces and make them appear in the final morphology.<sup>10</sup> Therefore, we speculate that the formation of one-dimensional nanobelts is possibly due to the growth along the *a*- or *b*-axis of a  $\text{Sb}_2\text{Te}_3$  crystal that is strongly restrained by AOT. In addition, the reaction time and temperature also have strong effects on the formation of the nanobelts. Further work to better understand the formation of  $\text{Sb}_2\text{Te}_3$  nanobelts is still in progress.

In summary, single-crystalline  $\text{Sb}_2\text{Te}_3$  nanobelts with the length of ca. 200  $\mu\text{m}$ , the width of 1–3  $\mu\text{m}$ , and the thickness of ca. 100 nm were successfully synthesized by a novel and convenient surfactant-assisted hydrothermal approach. The ionic surfactant AOT acted as the shape controller in the synthetic process. We believe that this synthetic route could be applied to obtain other low-dimensional semiconducting telluride nanostructures. Optimizations of the thermoelectric transport properties through assembly or doping of the  $\text{Sb}_2\text{Te}_3$  nanobelts may lead to novel thermoelectric materials and devices for applications.

**Acknowledgment.** The authors are grateful for the financial aid from the National Natural Science Foundation of China (Grant Nos. 20372060, 20340420326, 20490210, 206301040, and 20602035) and the MOST of China ("973" Program, Grant No. 2006CB601103).

**Supporting Information Available:** Detailed scheme of the synthetic process, EDS pattern, SEM image. This material is available free of charge via the Internet at <http://pubs.acs.org>.

## References

- (1) (a) Pan, Z. W.; Dai, Z. R.; Wang, Z. L. *Science* **2001**, *291*, 1947. (b) Yang, R.; Wang, Z. L. *J. Am. Chem. Soc.* **2006**, *128*, 1466. (c) Liu, J. F.; Li, Q. H.; Wang, T. H.; Yu, D. P.; Li, Y. D. *Angew. Chem., Int. Ed.* **2004**, *43*, 5048.
- (2) (a) Ma, C.; Moore, D.; Li, J.; Wang, Z. L. *Adv. Mater.* **2003**, *15*, 228. (b) Zhang, J.; Jiang, F. H.; Zhang, L. D. *J. Phys. Chem. B* **2004**, *108*, 7002.
- (3) (a) Jiang, Y.; Meng, X. M.; Yiu, W. C.; Liu, J.; Ding, J. X.; Lee, C. S.; Lee, S. T. *J. Phys. Chem. B* **2004**, *108*, 2784. (b) Joo, J.; Son, J. S.; Kwon, S. G.; Yu, J. H.; Hyeon, T. *J. Am. Chem. Soc.* **2006**, *128*, 5632.
- (4) (a) Zhang, J. L.; Du, J. M.; Han, B. X.; Liu, Z. M.; Jiang, T.; Zhang, Z. F. *Angew. Chem., Int. Ed.* **2006**, *45*, 1116. (b) Kang, Z. H.; Wang, E. B.; Mao, B. D.; Su, Z. M.; Gao, L.; Lian, S. Y.; Xu, L. *J. Am. Chem. Soc.* **2005**, *127*, 6534. (c) Mo, M. S.; Zeng, J. H.; Liu, X. M.; Yu, W. C.; Zhang, S. Y.; Qian, Y. T. *Adv. Mater.* **2002**, *14*, 1658.
- (5) (a) Xi, G.; Peng, Y.; Wan, S.; Li, T.; Yu, W.; Qian, Y. *J. Phys. Chem. B* **2004**, *108*, 20102. (b) Sigman, M. B.; Korgel, B. A. *J. Am. Chem. Soc.* **2005**, *127*, 10089.
- (6) (a) Christian, P.; O'Brien, P. *J. Mater. Chem.* **2005**, *15*, 4949. (b) Zou, H.; Rowe, D. M.; Min, J. *J. Vac. Sci. Technol. A* **2001**, *19*, 899. (c) ElMandouh, Z. S. *J. Mater. Sci.* **1995**, *30*, 1273. (d) Das, V. D.; Soundararajan, N.; Pattabi, M. *J. Mater. Sci.* **1987**, *22*, 3522.
- (7) (a) Hicks, L. D.; Dresselhaus, M. S. *Phys. Rev. B* **1993**, *47*, 12727. (b) Hicks, L. D.; Dresselhaus, M. S. *Phys. Rev. B* **1993**, *47*, 16631. (c) Venkatasubramanian, R.; Siivola, E.; Colpitts, T.; Quinn, B. O. *Nature* **2001**, *413*, 597.
- (8) (a) Wang, W. Z.; Poudel, B.; Yang, J.; Wang, D. Z.; Ren, Z. F. *J. Am. Chem. Soc.* **2005**, *127*, 13792. (b) Christian, P.; O'Brien, P. *J. Mater. Chem.* **2005**, *15*, 4949. (c) Garje, S. S.; Eisler, D. J.; Ritch, J. S.; Afzaal, M.; O'Brien, P.; Chivers, T. *J. Am. Chem. Soc.* **2006**, *128*, 3120. (d) Karkamkar, A. J.; Kanatzidis, M. G. *J. Am. Chem. Soc.* **2006**, *128*, 6002. (e) Jin, C. G.; Zhang, G. Q.; Qian, T.; Li, X. G.; Yao, Z. *J. Phys. Chem. B* **2005**, *109*, 1430. (f) Yang, J. Y.; Zhu, W.; Gao, X. H.; Bao, S. Q.; Fan, X.; Duan, X. K.; Hou, J. *J. Phys. Chem. B* **2006**, *110*, 4599.
- (9) (a) Liang, J. H.; Peng, C.; Wang, X.; Zheng, X.; Wang, R. J.; Qiu, X. P.; Nan, C. W.; Li, Y. D. *Inorg. Chem.* **2005**, *44*, 9405. (b) Wang, J. W.; Li, Y. D. *Chem. Commun.* **2003**, 2320. (c) Liu, Z. P.; Li, S.; Yang, Y.; Peng, S.; Hu, Z. K.; Qian, Y. T. *Adv. Mater.* **2003**, *15*, 1946.
- (10) (a) Li, F.; Ding, Y.; Gao, P.; Xin, X.; Wang, Z. L. *Angew. Chem., Int. Ed.* **2004**, *43*, 5238. (b) Yu, D. B.; Yam, V. W. W. *J. Am. Chem. Soc.* **2004**, *126*, 13200. (c) Im, H. S.; Lee, Y. T.; Wiley, B.; Xia, Y. N. *Angew. Chem., Int. Ed.* **2005**, *44*, 2154.

JA066944R